JOURNAL OF MATERIALS SCIENCE 30 (1995) 2675–2681

The growth characteristics of chemical vapour-deposited β-SiC on a graphite substrate by the $SiCl_4/C_3H_8/H_2$ system

T. T. LIN, M. H. HON
Department of Materials Science and Engineering (Mat. 32), National Cheng Kung University, Tainan, 70101, Taiwan

Silicon carbide has been grown at 1300–1800 °C by chemical vapour deposition using the $SiCl_4/C_3H_8/H_2$ system on a graphite substrate. The effect of C_3H_8 flow rate and deposition temperature on the growth characteristics and structure of the deposit has been studied. The experimental results show that the degree of film density is changeable from a dense plate to a porous one with increasing C_3H_8 flow rate. The activation energy increases with increasing C_3H_8 flow rate. The grain size of the polycrystalline β-SiC becomes coarser when the C_3H_8 flow rate and the deposition temperature are increased. The preferred orientation of the deposited SiC layers changes from (1 1 1) to (2 2 0) on increasing deposition temperature from 1300 °C to 1400 °C. The deposition mechanism is also discussed.

1. Introduction

Silicon carbide is considered to be a useful material for structural and electronic applications, because it has excellent physical, electronic and optical properties such as high-temperature stability, extreme hardness, wide energy band gap, high electron mobility, low neutron absorption and excellent resistance to chemical attack, etc. [1–3]. The β-SiC crystals have been grown by many investigators using the chemical vapour deposition (CVD) method [4–6]. The CVD silicon carbide coating on graphite is very interesting for many industrial applications such as heat exchangers, furnace resistors, nozzle materials, electrodes and so on, for protecting graphite substrate from oxidation at high temperature [7]. The SiC deposits obtained by thermal decomposition of methyltrichlorosilane (MTS) are widely employed [8–10], owing to the 1:1 ratio of carbon and silicon atoms contained in the reactant gas. The graphite substrate can remain stable at a very high temperature in a non-oxidative atmosphere, therefore, the gaseous precursor using silicon tetrachloride, propane and hydrogen ($SiCl_4/C_3H_8/H_2$) is feasible for high-temperature deposition. The characteristics of this reaction system are the high growth rate and separable inlet concentration of silicon and carbon atoms [11–13]. They can be well controlled to deposit a stoichiometric, silicon-rich or carbon-rich SiC layer. The main purpose of the present work is to understand the influence of the experimental parameters, C_3H_8 flow rate and temperature, on the morphology, the preferred orientation, the growth rate and the chemical compositions. The deposition mechanism is also discussed.

2. Experimental procedure

A cold-wall type CVD reactor was set up for the present work as illustrated in Fig. 1. Silicon carbide was deposited onto a graphite substrate under a low pressure (100 torr; 1 torr = 133.322 Pa) at 1300–1800 °C. The dimensions of the graphite substrate were 40 mm × 12 mm × 2 mm; the substrate was directly heated using an electric current. The precursors, $SiCl_4$ and C_3H_8, were used as silicon and carbon sources, respectively. The $SiCl_4$ vapour was carried from a saturator by maintaining the temperature at 0 °C, and the flow rate was controlled by adjusting the flow rate of bubbling hydrogen carrier gas. The deposition temperature was measured by an optical pyrometer. The detailed experimental parameters are shown in Table I. The thickness of the deposit and surface morphology were observed by scanning electron

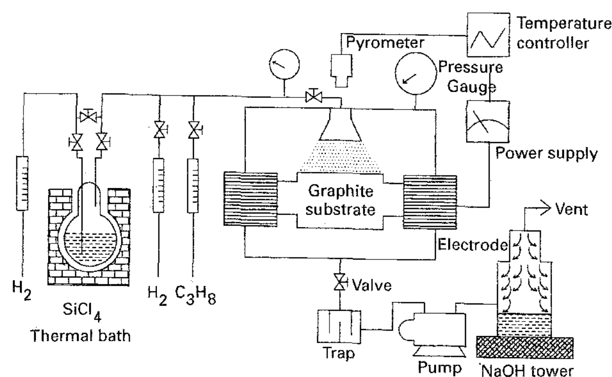

Figure 1 Schematic diagram of the experimental apparatus for CVD SiC.

0022–2461 © *1995 Chapman & Hall*

TABLE I List of experimental conditions

Total system pressure	100 torr
Deposition temperatures	1300–1800 °C
Deposition time	0.5 h
Flow rate of H_2	2000 standard $cm^3 min^{-1}$
Flow rate of C_3H_8	8–35 standard $cm^3 min^{-1}$
Flow rate of $SiCl_4$	120 standard $cm^3 min^{-1}$

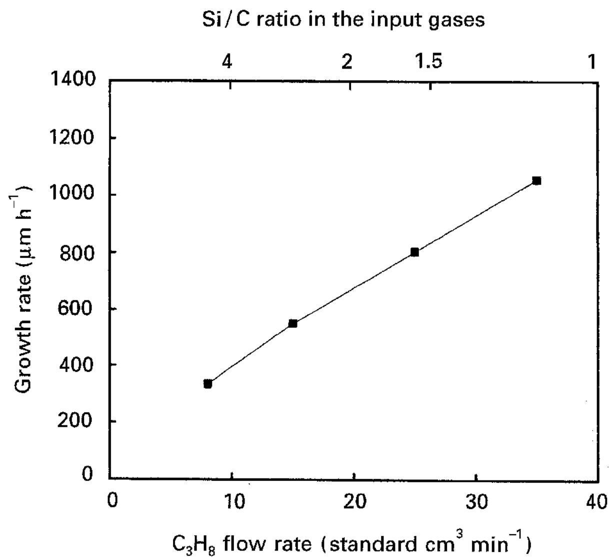

Figure 2 Effect of the C_3H_8 flow rate on the growth rate of SiC at 1500 °C.

microscopy. The crystal structure was analysed by X-ray diffraction and the degree of preferred orientation was calculated from the intensities of (1 1 1), (2 0 0) and (3 1 1) of the as-grown sample.

3. Results and discussion

3.1. Effects of C_3H_8 input concentration

The variation of the deposition rate with the C_3H_8 concentration is shown in Fig. 2. The deposition rate increases linearly with C_3H_8 concentration. It is well understood that the concentration of C_3H_8 in the boundary layer increases with increasing input concentration. This is the reason for the increasing SiC growth rate. The surface morphology is strongly dependent on the C_3H_8 concentration, as shown in Fig. 3. The faceted structure observed in Fig. 3a and b, occurs at lower C_3H_8 flow rate and the grain size of the SiC deposit with 15 standard $cm^3 min^{-1}$ C_3H_8 flow rate is larger than that of 8 standard $cm^3 min^{-1}$. The facet structure deposited at 25 standard $cm^3 min^{-1}$ C_3H_8 flow rate is small and the grain-size distribution is broad. The C_3H_8 flow rate increases up to 35 standard $cm^3 min^{-1}$ and the morphology changes from faceted structure to leaf-like structure as shown in Fig. 3d. Fig. 4 shows the cross-sectional fracture morphology of SiC deposited at different C_3H_8 concentrations. The dense plate was deposited at the C_3H_8 flow rate of 25 standard $cm^3 min^{-1}$, but

Figure 3 Effect of the C_3H_8 flow rate of (a) 8, (b) 15, (c) 25, (d) 35 standard $cm^3 min^{-1}$ on surface morphology at 1500 °C.

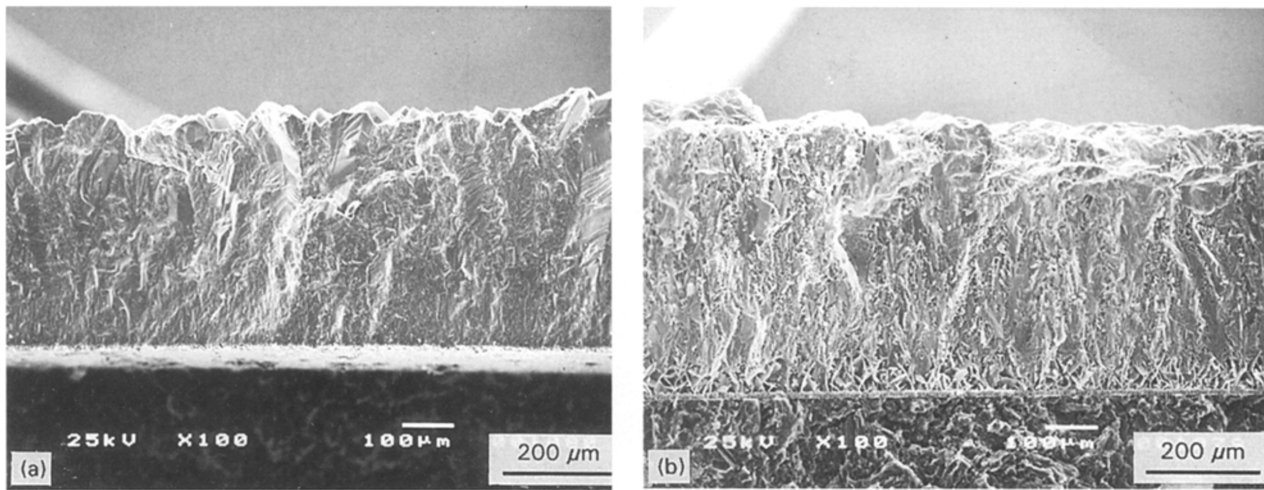

Figure 4 Scanning electron micrographs of cross-sectional fracture morphology at 1500 °C with different C_3H_8 flow rates of (a) 25 and (b) 35 standard $cm^3 min^{-1}$.

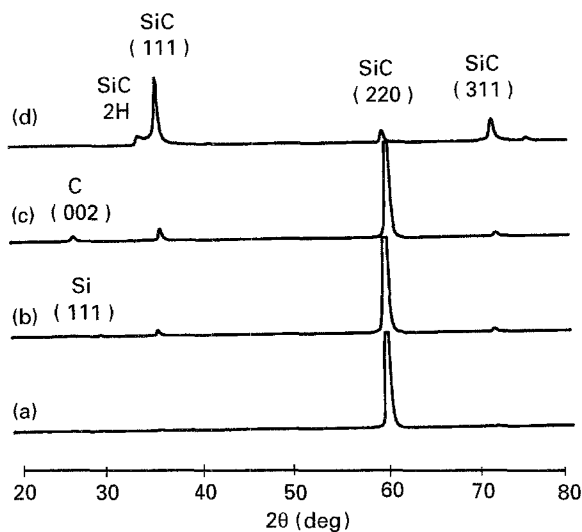

Figure 5 XRD diffraction patterns with various C_3H_8 flow rates of (a) 8, (b) 15, (c) 25, and (d) 35 standard $cm^3 min^{-1}$ at 1500 °C.

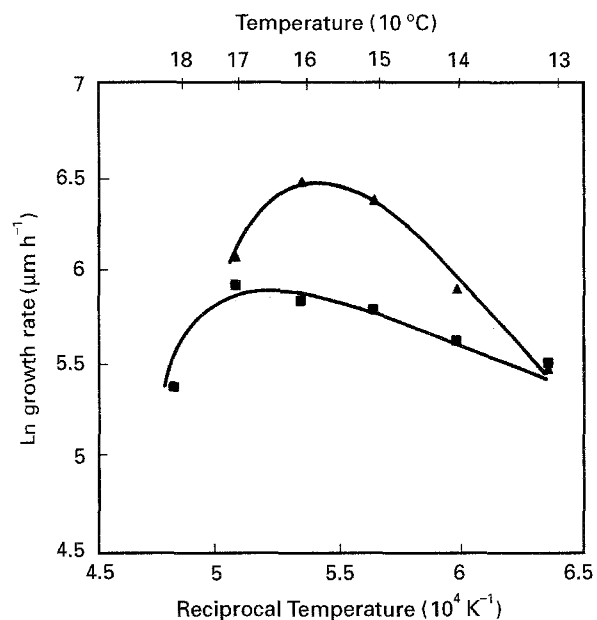

Figure 6 Effect of temperature on the growth rate with various C_3H_8 flow rates (■) 8 and (▲) 15 standard $cm^3 min^{-1}$.

the porous plate appears at 35 standard $cm^3 min^{-1}$. The porous structure is found through the deposited layer, but it is more serious near the substrate surface because the growth rate is fast at the beginning of deposition. Excess silicon peaks in Fig. 5 are observed in layers deposited at a C_3H_8 flow rate of 15 standard $cm^3 min^{-1}$ and excess carbon peaks are observed in the layer deposited at a C_3H_8 flow rate of 25 standard $cm^3 min^{-1}$. The 2H structure of α-polytype SiC is found at 35 standard $cm^3 min^{-1}$. From the calculation of the phase diagram of silicon carbide for thermodynamic equilibrium it is found that as the atomic ratio of the Si/C inlet gas increases to 1.5 the SiC + C phase is co-deposited at 1500 °C and 100 torr which agrees with our results [14].

3.2. Effects of deposition temperature

The dependence of SiC growth rate on the deposition temperature is stronger for a higher C_3H_8 flow rate than a lower one, as shown in Fig. 6. By calculation for the Arrhenius equation the apparent activation

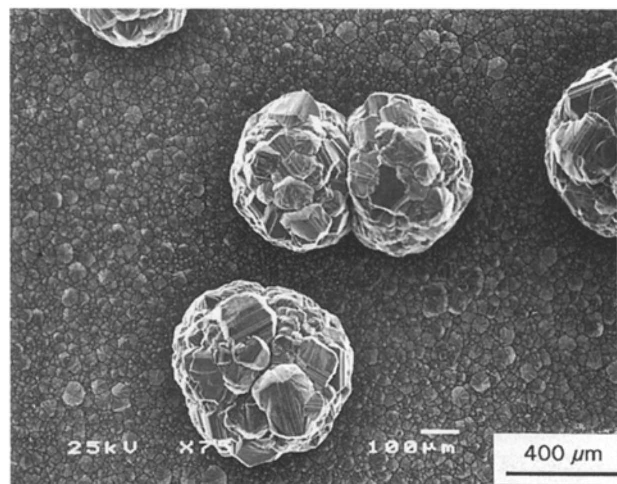

Figure 7 Scanning electron micrograph of homogeneous nucleation particles (1700 °C, 8 standard $cm^3 min^{-1}$ for C_3H_8 flow rate).

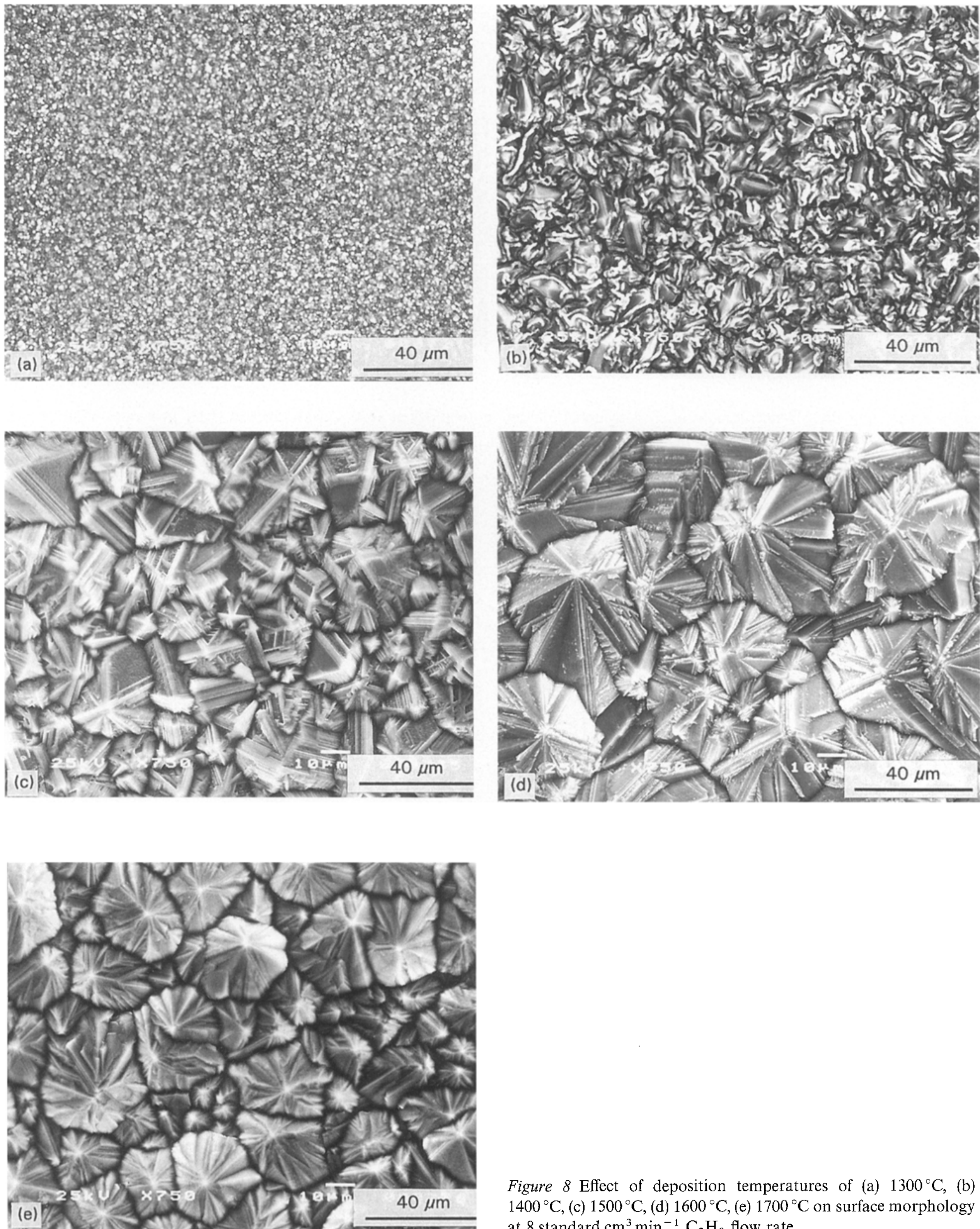

Figure 8 Effect of deposition temperatures of (a) 1300 °C, (b) 1400 °C, (c) 1500 °C, (d) 1600 °C, (e) 1700 °C on surface morphology at 8 standard $cm^3 min^{-1}$ C_3H_8 flow rate.

energies corresponding to low and high C_3H_8 flow rates are 6.1 and 21.2 $kcal mol^{-1}$, respectively. The value of the former is rather small compared with the value of 35 $kcal mol^{-1}$ obtained by Keneko and Okuno [15]. Owing to the low activation energy, a diffusion control is proposed for the deposition process. The growth rate decreases at higher temperature due to homogeneous nucleation and thermal etching in the diffusion layer as often found in the CVD reaction [16]. A homogeneous nucleation particle is seen in Fig. 7 deposited at 1700 °C or higher and 8 standard $cm^3 min^{-1}$ C_3H_8 flow rate and the growth rate decreases. At 1800 °C and 15 standard $cm^3 min^{-1}$ C_3H_8 flow rate, there is no silicon carbide deposited on the substrate because the homogeneous nucleation and thermal etching are very serious at high temperature. At high C_3H_8 flow rate, the homogeneous nucleation appears at lower temperature, which is attributed to the high concentration of C_3H_8 colliding more easily to nucleate in the gas phase.

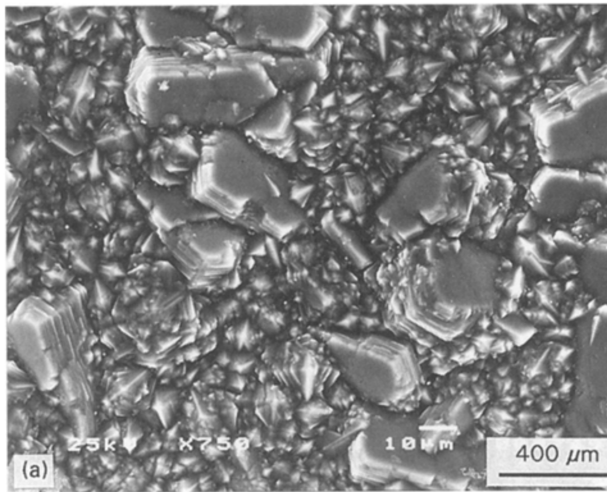

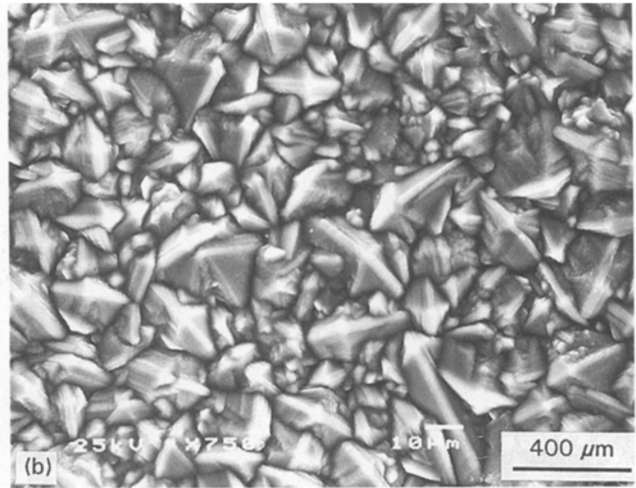

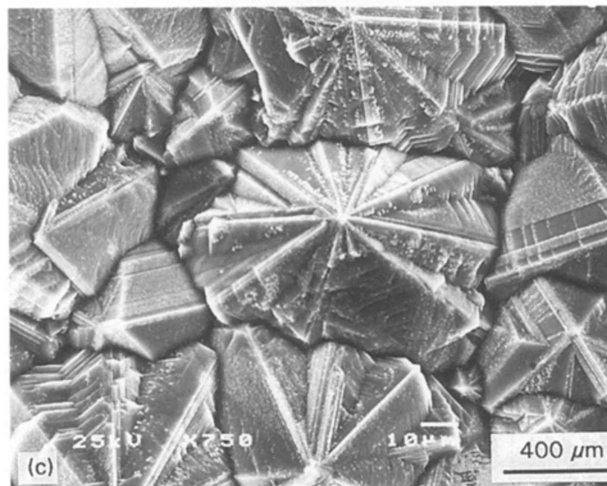

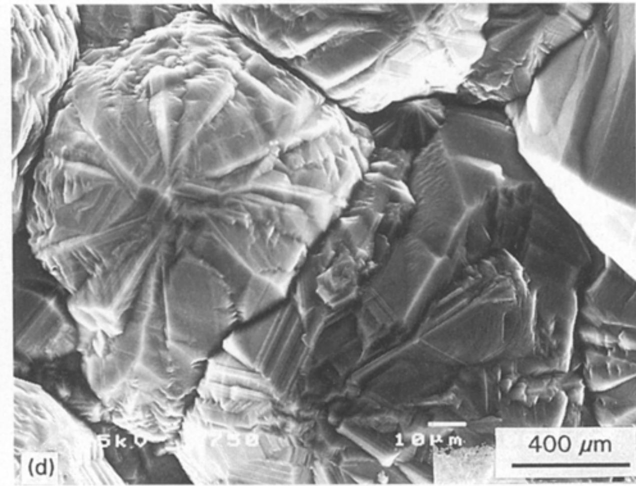

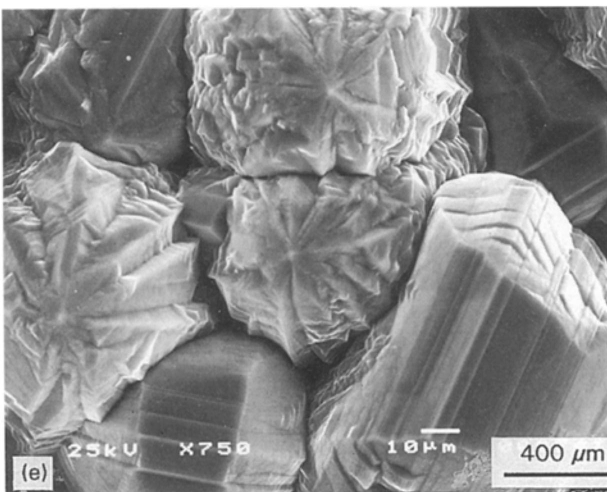

Figure 9 Effect of the deposition temperatures of (a) 1300 °C, (b) 1400 °C, (c) 1500 °C (d) 1600 °C, (e) 1700 °C on surface morphologies at 15 standard $cm^3 min^{-1}$ C_3H_8 flow rate.

The surface morphology of SiC deposited at different temperatures and C_3H_8 flow rates is shown in Figs 8 and 9. Smooth, featureless, angular and strongly faceted crystals are obtained in the deposits by varying the deposition temperature. The crystal size of SiC increases with both increasing deposition temperature and C_3H_8 flow rate. The dependence of crystal size on the deposition temperature may be ascribed to the high surface mobility of reaction atoms at high temperature resulting in the formation of a large crystal size. The crystal size of SiC deposited at 1700 °C in Figs 8e and 9e is decreased due to the homogeneous nucleation reducing the surface concentration of the substrate. The surface morphology is featureless in Fig. 8a but granular in Fig. 9a, due to the different C_3H_8 flow rate.

Fig. 10 shows the fractured morphology of samples deposited at 1300 and 1500 °C, respectively. The layer deposited at 1300 °C has a dense and smooth fracture surface, whereas the layer deposited at 1500 °C shows a typical columnar structure.

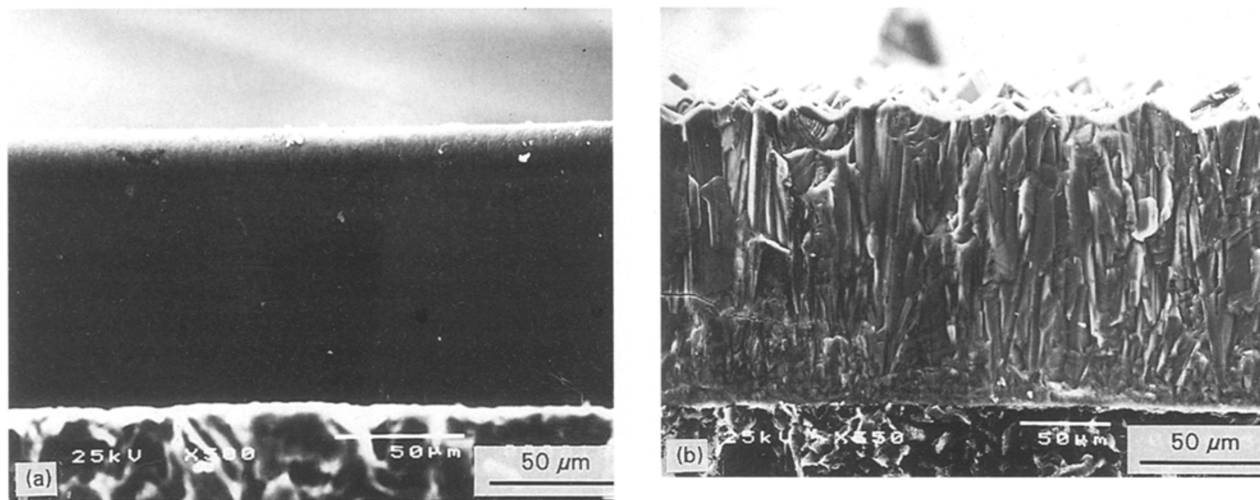

Figure 10 Scanning electron micrographs of cross-sectional fracture morphology with different deposition temperatures: (a) 1300 °C and (b) 1500 °C at 8 standard $cm^3 min^{-1}$ C_3H_8 flow rate.

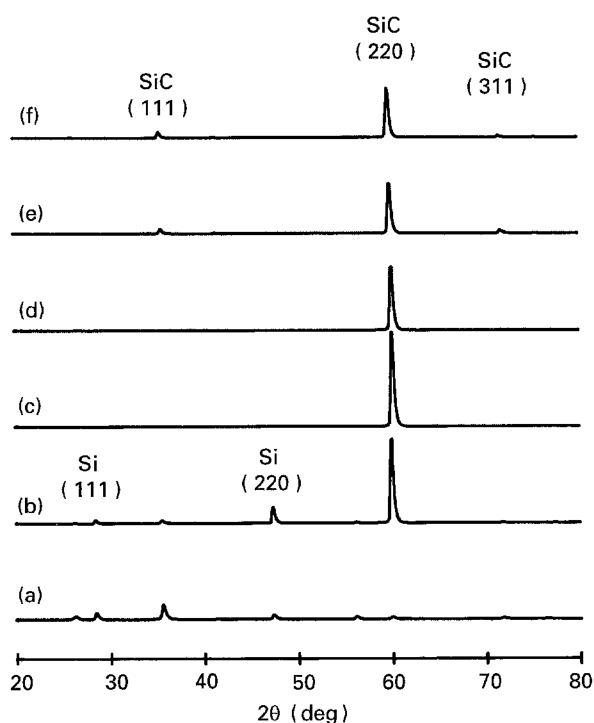

Figure 11 XRD diffraction patterns with various deposition temperatures of (a) 1300 °C, (b) 1400 °C, (c) 1500 °C, (d) 1600 °C, (e) 1700 °C at 8 standard $cm^3 min^{-1}$ C_3H_8 flow rate.

3.3. Crystallography, texture and growth mechanism

The XRD patterns of samples deposited at different temperatures are shown in Fig. 11. Excess silicon peaks are observed in layers deposited at 1300 and 1400 °C, and the peak intensities of excess silicon decrease with increasing deposition temperature. The SiC single phase without excess silicon appears at 1500 °C deposition.

The texture of β-SiC layers obtained by the CVD process is strongly dependent on the process parameters, especially the deposition temperature. The preferred orientation of a certain crystal plane $(h\,k\,l)$ in polycrystalline deposits is described by the texture coefficient (TC) using the Harris method [17]

$$\mathrm{TC} = \frac{(I/I_0)}{(1/n)\Sigma (I/I_0)_i} \qquad (1)$$

where I is the measured intensity, I_0 is the ASTM standard intensity, and the n is the number of reflection. The texture coefficients of films deposited at different temperatures are shown in Fig. 12. The SiC (1 1 1) texture grows favourably at low temperature (1300 °C) and the SiC (2 2 0) texture prefers at high temperature (above 1400 °C), which the surface-adsorbed atoms have sufficient energy to migrate to the stable sites. The accumulation of adsorbed atoms to form a growing front has a better chance to increase by capturing species in the diffusion layer. When the temperature increases to 1700 °C, the homogeneous nucleation reaction dominates in the deposition and the (2 2 0) texture coefficient decreases, but the (1 1 1) and (3 1 1) texture coefficients increase.

The faceted structure has a clear multi-twin star configuration and re-entrant corners as shown in Figs 8 and 9. Fig. 13 shows the twin lines on deposited SiC after thermal etching at 1800 °C. These features

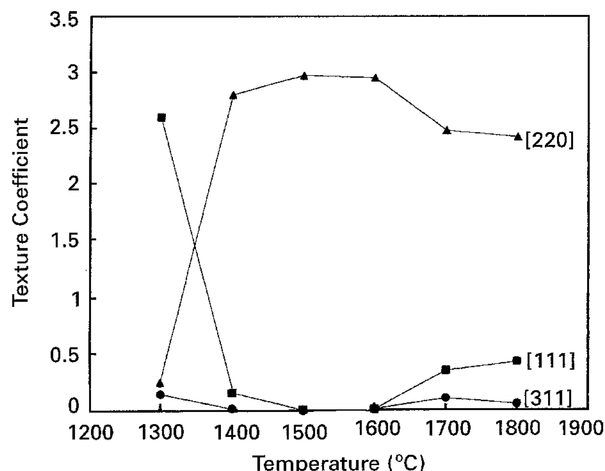

Figure 12 Effect of deposition temperatures on texture coefficient at 8 standard $cm^3 min^{-1}$ C_3H_8 flow rate.

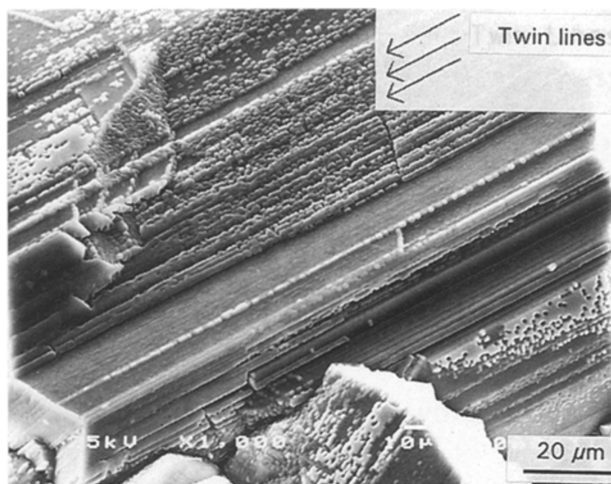

Figure 13 Scanning electron micrograph of twin lines in deposited SiC by thermal etching.

indicate that re-entrant twin acts as an important role for the SiC growth in the CVD process [18].

4. Conclusions

β-SiC deposition on graphite by reduced pressure CVD using the $SiCl_4/C_3H_8/H_2$ system has been investigated. The relations between deposition parameters and growth characteristics of SiC layers were examined by SEM and X-ray. The results are summarized as follows.

1. The crystallographic structure of SiC layers deposited is almost polycrystalline β-SiC, except that a small amount of 2H structure of α-polytype SiC appears at a high C_3H_8 flow rate.

2. The porous SiC plate was obtained at 35 standard $cm^3 min^{-1}$ C_3H_8 flow rate and the dense plate appears at a lower flow rate.

3. At a deposition temperature of 1300–1600 °C and 8 standard $cm^3 min^{-1}$ C_3H_8 flow rate, the deposition rate limitation is controlled by diffusion. The activation energy increases from 6.1 kcal mol^{-1} to 21.2 kcal mol^{-1} as the C_3H_8 flow rate increases from 8 to 15 standard $cm^3 min^{-1}$. The homogeneous nucleation appears at about 1700 °C and a high C_3H_8 concentration lowers the homogeneous nucleation temperature.

4. The free silicon is co-deposited with β-SiC at a temperature lower than 1500 °C. The free silicon content decreases with increasing deposition temperature.

5. The grain size increases with increasing deposition temperature and C_3H_8 flow rate.

6. The texture of SiC layers is (1 1 1) at 1300 °C. The (2 2 0) texture coefficient increases with deposition temperature but decreases after homogeneous nucleation appears, whereas the (1 1 1) and (3 1 1) texture coefficients change oppositely. The multi-twin star structures are observed in many SiC deposits. The results indicate that re-entrant twins have an important role in the SiC growth in the CVD process.

Acknowledgement

The authors thank the National Science Council, Taiwan for support under contract NSC80-04051006-33.

References

1. R. J. PRICE, *Ceram. Bull.* **48** (1969) 859.
2. R. C. MARSHALL, J. W. FAUST and JR. C. E. RYAN (eds), "Silicon Carbide" (University of South Carolina Press, Columbia, SC, 1973) p. 668.
3. K. SASAKI, E. SAKUMA, S. MISAWA, S. YOSHIDA and S. GONDA, *Appl. Phys. Lett.* **45** (1984) 72.
4. J. CHIN, P. K. GANTZEL and R. G. HUDSON, *Thin Solid Films* **40** (1977) 57.
5. D. P. STINTON and W. J. ACKEY, *Ceram. Bull.* **57** (1978) 568.
6. H. G. LIPON, in "Silicon Carbide–A High Temperature Semiconductor", edited by J. R. O'Connor and J. Smilthens (Pergamon Press, Oxford, 1960) p. 371.
7. J. SCHLICHTING, *Powder Met. Int.* **12** (1980) 141.
8. M. G. SO and J. S. CHUN, *J. Vac. Sci. Technol.* **A6** (1988) 5.
9. B. T. CHOI and D. R. KIM, *J. Mater. Sci. Lett.* **10** (1991) 860.
10. Y. M. LU and M. H. HON, *Nippon Seramikkusu Kyokai Gakujutsu Ronbunshi* **99** (1991) 1175.
11. T. HIRAI, T. GOTO and T. KAJI, *Yogyo-Kyokai-Shi* **91** (1983) 503.
12. H. MATSUNAMI, S. NISHINO and T. TANAKA, *J. Crystal Growth* **45** (1978) 138.
13. A. PARRETTA, A. CAMANZI, G. GIUNTA and A. MAZZARANO, *J. Mater. Sci.* **26** (1991) 6057.
14. Y. WANG, M. SASAKI, T. GOTO and T. HIRAI, *ibid.* **25** (1990) 4607.
15. T. KENEKO and T. OKUNO, *J. Crystal. Growth* **91** (1988) 599.
16. A. W. C. VAN KEMENADE and C. F. STEMFOORT, *ibid.* **12** (1972) 13.
17. C. BARRET and T. B. MASSALSKI, "Structure of Metals" (Pergamon, Oxford, 1980) p. 204.
18. D. J. CHENG, W. J. SHYY, D. H. KUO and M. H. HON, *J. Electrochem. Soc. Solid State Sci. Technol.* **134** (1987) 3145.

Received 3 December 1993
and accepted 4 October 1994